Preconscious Prediction of a Driver's Decision Using Intracranial Recordings

Omri Perez[1], Roy Mukamel[1], Ariel Tankus[2,3], Jonathan D. Rosenblatt[4], Yehezkel Yeshurun[1], and Itzhak Fried[1,2,5]

Abstract

■ While driving, we make numerous conscious decisions such as route and turn direction selection. Although drivers are held responsible, the neural processes that govern such decisions are not clear. We recorded intracranial EEG signals from six patients engaged in a computer-based driving simulator. Patients decided which way to turn (left/right) and subsequently reported the time of the decision. We show that power modulations of gamma band oscillations (30–100 Hz) preceding the reported time of decision (up to 5.5 sec) allow prediction of decision content with high accuracy (up to 82.4%) on a trial-by-trial basis, irrespective of subsequent motor output. Moreover, these modulations exhibited a spatiotemporal gradient, differentiating left/right decisions earliest in premotor cortices and later in more anterior and lateral regions. Our results suggest a preconscious role for the premotor cortices in early stages of decision-making, which permits foreseeing and perhaps modifying the content of real-life human choices before they are consciously made. ■

INTRODUCTION

The neural signature preceding voluntary action was first addressed by Libet and colleagues (Libet, Gleason, Wright, & Pearl, 1983) who showed that a slow negative potential recorded at the scalp actually began before the conscious will to perform a voluntary act as reported by human participants. This slow negativity, originally described by Kornhuber and Deecke, is referred to as the readiness potential or Bereitschaftspotential (Shibasaki & Hallett, 2006; Kornhuber & Deecke, 1965) and most likely originates from the SMA (Haggard, 2008; Shibasaki & Hallett, 2006). The fact that this recurring signal can be detected before the reported time of the conscious intention to act (by an average of 350 msec) stimulated much debate (Gomes, 2007, 2010; Lavazza & De Caro, 2009; Trevena & Miller, 2009; Haggard, 2005, 2008; Soon, Brass, Heinze, & Haynes, 2008; Brass & Haggard, 2007; Libet, 2004; Wegner, 2003; Gomes, 1998; Keller & Heckhausen, 1990; Libet, Gleason, et al., 1983; Libet, Wright, & Gleason, 1983). Recently, it has been demonstrated that it is possible to decode the content of a conscious decision using spatial patterns of the fMRI signal up to 4–7 sec before the decision is made, although the decoding accuracy was relatively low (Soon, He, Bode, & Haynes, 2013; Soon et al., 2008; Haynes et al., 2007). This could mean that not only the decision to act but also the specifics of the decision are present in the brain before the conscious decision is experienced and reported (Soon et al., 2008, 2013). A central challenge in the interpretation of most of these studies (Trevena & Miller, 2009; Soon et al., 2008; Haggard & Eimer, 1999; Libet, Gleason, et al., 1983) is the potential confounding of decision content by motor plan. For example, in some studies (Trevena & Miller, 2009; Soon et al., 2008; Haggard & Eimer, 1999), the participant was instructed to decide when and with which hand to press a button. Thus, the intention decoded from the participant's neural activity could have been partially related to motor preparation and not to the intention per se (as suggested by Soon et al., 2013; Hampton & O'Doherty, 2007; Haynes et al., 2007). However, it should be noted that Soon et al. (2013) explicitly decoupled abstract intentions from motor plans and actions. Similarly, we specifically designed the current electrophysiological study to address this challenge.

In the current study, we sought to identify the earliest neural correlates of a decision and examine whether these neural correlates enable us to predict the content of the pending decision on a trial-by-trial basis. On the basis of extant studies, we hypothesized that the decision to act arises from the temporal integration of frontoparietal activity (Soon et al., 2013; Fried, Mukamel, & Kreiman, 2011; Haggard, 2011; Desmurget et al., 2009; Desmurget & Sirigu, 2009; Matsuhashi & Hallett, 2008; Assal, Schwartz, & Vuilleumier, 2007; Gold & Shadlen, 2007; Sirigu et al., 2004; Libet, Gleason, et al., 1983).

[1]Tel Aviv University, [2]University of California Los Angeles, [3]Technion – Israel Institute of Technology, [4]Weizmann Institute of Science, Rehovot, Israel, [5]Tel Aviv Sourasky Medical Center

Journal of Cognitive Neuroscience 27:8, pp. 1492–1502
doi:10.1162/jocn_a_00799

We recorded intracranial EEG (iEEG) signals directly from the human cortex in neurosurgical patients with intracranial electrodes implanted for clinical reasons. The patients engaged in a driving simulator where, every time the car approached a junction, the patient had to decide which way to turn and then report the time of decision.

The experiment was designed to disambiguate the decision-making process from the process of motor planning (Lavazza & De Caro, 2009) by denying the participants the prior knowledge of which key will turn the car in the desired direction (Hampton & O'Doherty, 2007; Haynes et al., 2007; see Methods and Figure 1).

We show that modulation of gamma band power during left and right decision trials detected electrodes that consistently distinguished between the two. Furthermore, we show that we are able to classify the decision content (left/right) and timing on a trial-by-trial basis.

METHODS

Participants

The study included six (n = 6) epileptic patients implanted with subdural iEEG electrodes (median age = 35 years, range = 25–39 years, five women). These patients have pharmacologically intractable epilepsy and were implanted with subdural iEEG electrodes aimed at evaluating the possibility of surgery. Electrode location was based solely on clinical criteria (Privman et al., 2007). Two patients were left handed and had medial–frontal epileptic foci (P05 and P06). The remaining four patients were right handed and had nonfrontal epileptic foci. Patients had normal or corrected-to-normal vision. The patients provided written informed consent to participate in the experiment. The Tel Aviv Sourasky Medical Center committee for activities involving human subjects approved the experimental protocol.

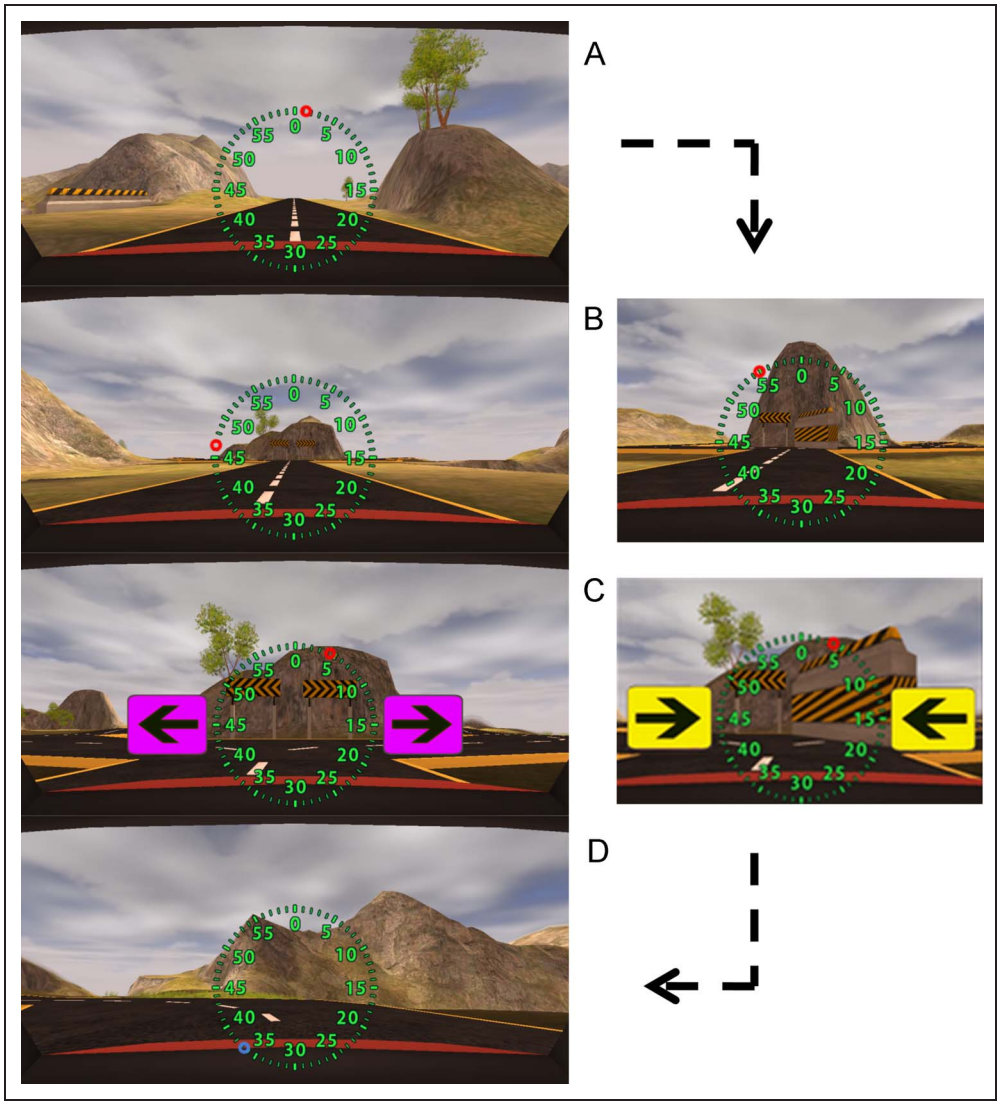

Figure 1. Screenshots from the simulator showing the flow of the Experiment. (A) Every trial starts when the junction is not yet visible. (B) After about 6 sec of driving, the junction, either free or blocked to the left or right, appears. (C) When reaching the junction, the key mapping arrows appear. Purple arrows denote "congruent" key mapping (i.e., pressing the button with the right hand turns the car to the right and pressing a different button with the left hand turns the car to the left). Yellow arrows indicate inversed key mapping (i.e., right hand for turning car left and left hand for turning car to the right). This late appearance of the mapping denies the patient of prior knowledge of which key will turn the car in the desired direction. The patient makes the decision in the time between B and C (this period is, on average, 12 sec). (D) After pressing the appropriate key according to the chosen direction, the patient specifies the location of the dot on the clock at the time of decision (each revolution of the clock is equal to 18 sec).

Materials

For the experiment, we programmed a driving simulator in-house using the Torque Game Engine (GarageGames, Eugene, OR). The car drives autonomously but requires input indicating where to turn at junctions by pressing either the left or right key with the matching index finger. Upon reaching the junction, a mapping signal informs of the mapping of the keys, either congruent (see Figure 1C) or inversed. This is to prevent the participant from generating a specific motor plan. On ~30% of the trials, one of the sides of the junction is randomly blocked by a large obstruction (see Figure 1B and C). This discourages the participant from making a motor decision before seeing the junction or from forming a response bias. From the moment the mapping signal appears, the participants had 5 sec to respond; if no response was given, then the trial was restarted.

We instructed the patients to decide before reaching the junction. As in previous studies, we also instructed the patients to decide freely and without any obvious pattern (Soon et al., 2008; Haggard & Eimer, 1999).

The simulator includes a clock face with a dot encircling it (Libet, Wright, et al., 1983). The angular velocity of the dot is 20° per second or 18 sec for a full revolution. After reaching the junction and indicating where to turn, the patient is instructed to shift the dot back to the location in which it was when he or she first became conscious of the decision (W, see Figure 1D). The period between the appearance of the junction and actual arrival at the junction is, on average, 12 sec long, and it is during this time that the participant is supposed to make the mental decision of where to turn.

Procedure

We conducted all sessions at a patient's quiet bedside while the patient was sitting upright in bed. Each patient participated in several sessions, totaling 36–67 trials. Within the "free" trials, the patients chose to turn "left" in 32–66.7% of the trials (median = 48%). At the end of the sessions, we debriefed the patients.

Data Acquisition

Initially, the study included eight patients (n = 8, P01–P08), but we discarded two patients (P01 and P07) because of clinical time constraints preventing them from performing a minimum of 10 trials in the task. In total, 257 iEEG electrode-recording sites were obtained from the remaining six patients. Electrode locations were based solely on clinical criteria by which the patients were implanted with subdural electrode strips and/or grids (Adtech, Racine, WI). Two patients had right hemispheric electrode locations, three had bilateral electrodes, and one had left hemispheric electrodes. The spatial coverage of the electrodes included frontal (48.2%), temporal (33.5%), parietal (12.8%), and occipital (5.4%) cortices. Each electrode was 2 mm in diameter, with 8-mm spacing. We used monopolar recordings referenced to an extracranial electrode sampled at 200 Hz and filtered between 1 and 100 Hz by the clinical equipment (Grass Technologies, West Warwick, RI). We determined the electrode Talairach locations by coregistration of CT scans with preoperative MRI, using iPlan Stereotaxy software (BrainLAB, Westchester, IL).

To remove noise generated by the external reference, we subtracted the average voltage across the electrodes in each time sample (common average reference) and notch filtered the signal at 50 Hz (the mains frequency in Israel).

Data Analysis

We performed the data analysis using Matlab (The Mathworks, Natick, MA). All analyses were performed per patient. The data pertaining to each trial were locked to the reported time of decision (W). We performed all analyses on "free" trials, that is, trials with an unobstructed junction.

Spectrograms

We generated event-related spectrograms for each patient and electrode using the approach outlined in Delorme and Makeig (2004). First, we Stockwell-transformed (Stockwell, Mansinha, & Lowe, 1996) all trials to produce the spectral estimate $F_k(f, t)$ of trial k at frequency f (1–100 Hz) and time t (−6 to 1 sec in relation to W; $\Delta t = 5$ msec, which corresponds to a sampling rate of 200 Hz). For each trial, we computed the spectral estimate of the baseline as well, $B_k(f, t)$ of trial k at frequency f (1–100 Hz) and time t (0–3 sec at the start of the trials; see Figure 1A). Next, we calculated the mean (across time and trials) log power baseline spectral estimate:

$$B(f) = \frac{10}{nT}\sum_{k=1}^{n}\sum_{t=1}^{T}\log_{10}\left(B_k(f,t)^2\right)$$

and the mean (across trials) log power spectrogram of the trials:

$$F(f,t) = \frac{10}{n}\sum_{k=1}^{n}\log_{10}\left(F_k(f,t)^2\right)$$

Finally, we subtracted the two to get a baseline-normalized decibel scale event-related spectrogram,

$$SPECT(f,t) = F(f,t) - B(f)$$

as seen in Figure 2.

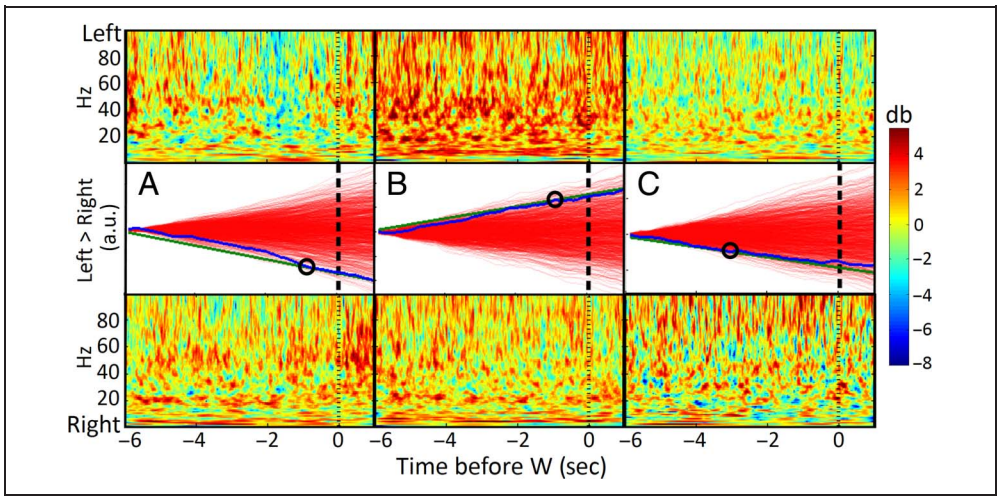

Figure 2. The relationship between the average spectrograms for each choice and the CUMSUM analysis. Each column shows for a single electrode the average spectrogram for decisions to turn left and right (top and bottom, respectively) and the CUMSUM analysis (middle). Zero seconds is the time of reported decision (W, black dashed lines), and the red lines represent the 1,000 CUMSUM traces calculated with permutated trial labels. Significance of the CUMSUM is estimated by the proportion of permutation CUMSUMs that cross the bounding line (green; see Methods). The black circle marks the significance time, that is, the point where the bounding line intersects the observed time course. (A) A right inferior frontal (Brodmann's area [BA] 47; P02) electrode. These spectrograms demonstrate higher gamma power preceding right decisions. In addition, the CUMSUM significantly tends to the bottom, that is, the right decision trials had, on average, higher gamma power around the significance time (intersection point between the observed CUMSUM and the bounding line) of the electrode. (B) A right inferior frontal (BA 44; P02) electrode. These spectrograms show an increased average gamma activity for left decisions, and the CUMSUM significantly tends to the top, which is related to higher gamma power in left choice trials. (C) A left premotor (BA 6; P06) electrode. The spectograms show increased gamma activity for right decisions, and accordingly, the CUMSUM significantly tends to the bottom.

Cumulative Sum Analysis

To test for the existence and timing of significant differences between left and right decisions, we employed a cumulative sum of differences (CUMSUM) analysis. We performed this analysis for each electrode in each patient. First, we filtered the signal in each trial, spanning 6 to 0 sec before W, to the gamma band, that is, 30–100 Hz (Basar, Basar-Eroglu, Karakas, & Schürmann, 2001). We then Hilbert transformed these filtered trial time courses to estimate instantaneous amplitude (Oppenheim & Schafer, 2009). This step eliminated the phase component of the signal, which is unlikely to be synchronized across trials because of behavioral timing inaccuracies. Next, for each condition (left and right decisions), we generated a grand-averaged time course,

$$G(t)_{c\in\{\text{Left,Right}\}} = \frac{1}{n_c}\sum_{\text{trial}\in c} x(t)$$

where $x(t)$ is the filtered and Hilbert-transformed time course, c is the set of trials of the current condition (left/right), and n_c is the number of trials in the current condition.

Then, to overcome timing inaccuracies because of behavioral variance, we binned the grand averages using 100-msec bins. We then normalized each of the two averaged time courses to the baseline by subtracting the mean value calculated for a period of 1 sec spanning 6.5 to 5.5 sec before W. Next, at each time bin, we calculated the instantaneous difference between the left and right grand-averaged time courses,

$$Diff(t) = GBinNorm(t)_{\text{Left}} - GBinNorm(t)_{\text{Right}}$$

where GBinNorm(t) is the binned and baseline normalized grand average time course of each condition. Finally, from this instantaneous difference time course, we generated a cumulative sum time course: $CUMSUM(t) = \sum_{i=t_0}^{t} Diff(i)$.

We selected the CUMSUM approach because of two main reasons: First, inspecting time course differences from a cumulative approach is compatible with the hypothesis that conscious action intention arises from accumulation of neural activity. Second, comparing the average gamma-power difference at every time bin would necessitate correcting for multiple comparisons at the single electrode level.

To estimate the significance of the CUMSUM of the left–right difference time course, we generated 1,000 CUMSUMs calculated in the same way but with permutated labels. We then fit a bounding line to the observed CUMSUM and derived the p value by counting the number of permutation CUMSUMs that cross the fitted line. We define the time of significance to be the intersection point between the fitted line and the observed CUMSUM (see Figure 2). This allowed us to identify, for each participant, the electrodes in which the gamma activity significantly differentiated between left and right decisions and at what time point. We tested the electrodes for significance using two thresholds: $\alpha = 0.05$ uncorrected and $q = 0.05$ within-subject false discovery rate (FDR, $q = 0.05$) multiple comparison correction (see Figure 3).

We defined the bounding line as $y = at + b$ where t is time relative to W, a is the slope, and b is the intercept. First, we calculated the intercept, $b = k \cdot \sigma(obs)$ where σ(obs) is the standard deviation of the observed CUMSUM

of differences time course described above and k is a constant. We set $k = 3.75$ as defined in a parametric sequential test aimed at detecting an effect size (μ/σ) of 1.4 at $\alpha = 0.01$ (Hedgcock, Crowe, Leuthold, & Georgopoulos, 2009; Armitage, 1975). We then determined the minimal slope such that the resulting line still bounded the observed CUMSUM time course:

$$\min\{a \mid |CUMSUM(t)| \le at + b \text{ for } t \in [-6, 0]\}$$

The significance time of the electrodes might be sensitive to the parametrization of the bounding line, specifically to the selection of the intercept. We thus attempted to estimate the magnitude of this sensitivity. For every significant electrode, we methodically shifted the intercept from 0% to 500% of its original value in 5% increments. For every such shifted intercept, we calculated the appropriate bounding line and intersection point (i.e., significance time). We then estimated the variance of the resulting differences between these times and the previously calculated significance time and computed the ratio between this and the maximally possible variance (the ratio can take values in the range [0, 1]). A low ratio indicates high certainty of the electrode's timing. When considering all of the significant electrodes, the range of the ratios is [0, 0.81], and the median is 0.06. We repeated this procedure to estimate the variance in the p values of the significant electrodes and in the angle of the resulting gradient described below. The range of p value changes from the observed is [−0.02, 0.3], the median is 0.005, and the *SD* is 0.055. To estimate the variance of the angle of the gradient described below, we randomly sampled 1,000 shifted-intercept significance times from the significant electrodes. For each such sample, we estimated the angle of gradient. The resulting median absolute angle change in degrees from the observed angle (80.1°) is 9.6°, and the *SD* is 17.1°. None of the angle changes were above 90°, hence there were no periodicity effects to account for.

To quantify the visual impression that there is a certain spatiotemporal pattern in the CUMSUM results, we show a scatter plot of the location of the electrodes versus their significance time. Because the apparent direction of the flow appears not to be along one of the main axes, we chose a rotated x (or Talairach y) axis and performed a grid search for the rotation angle that maximized the correlation of the electrode locations, along the rotated x axis, with their significance time. The angle of rotation that maximized this correlation was found to be $\theta = 80.1°$ ($r^2 = .325$, $p < .001$). We calculated the new coordinates as follows $x' = x \cdot \cos(\theta) - y \cdot \sin(\theta)$. The resulting axis is approximately parallel to the gradient shown in Figure 3C. We then used these new x' coordinates to create the scatter plot shown in Figure 3B. Thirty-four significant frontal electrodes are presented in the aforementioned scatter plot. We did not include the remaining 24 significant electrodes because they were either too medial (not visible in Figure 3) or not in the frontal lobe.

This exhaustive grid search for the maximum correlation implies that the significance value ($r^2 = .325, p < .001$) of the resulting correlation is potentially an overestimate. We thus estimated the significance of the gradient using a permutation test in which we permuted the time of significance of the electrodes. For each permutation ($n = 1{,}000$), we searched for the rotation that yields the maximal correlation. Then, we compared the observed correlation coefficient to this null distribution to yield the p value.

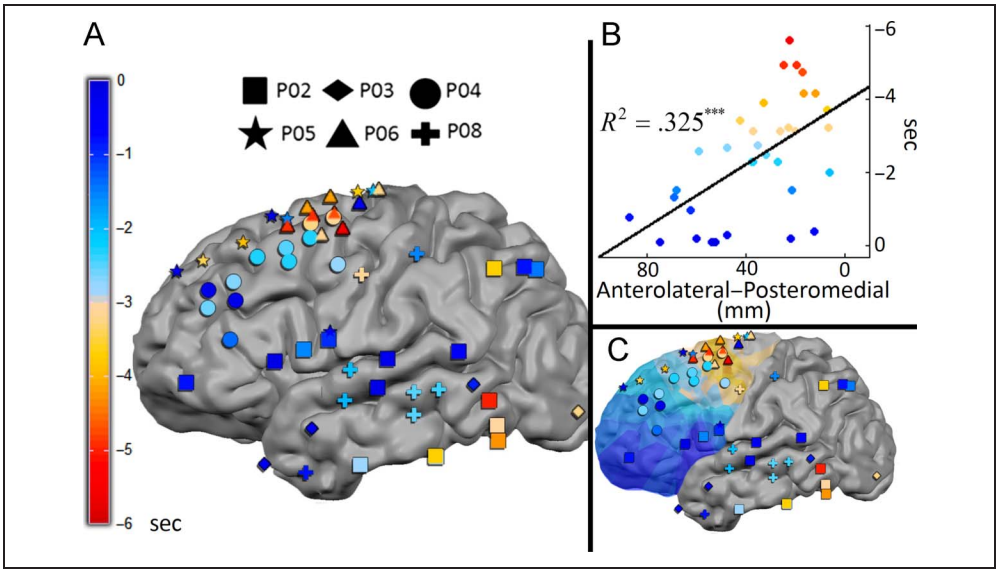

Figure 3. The spatiotemporal distribution of the electrodes with the cumulative sum of gamma power significantly distinguishing between decisions to turn left or right. (A) Symbols denote significant ($p < .05$ uncorrected) electrodes in specific patients. Colors signify the time in relation to W of the electrodes' significance times. (B) A scatter plot showing the relationship between the locations of the electrodes along an axis rotated in a dorsomedial to anterolateral direction and the electrodes' significance times. (C) A frontal lobe spatiotemporal gradient with a direction similar to the axis in B. For the entire results including the electrodes that are not significant and information regarding the estimation accuracy of the significance times.

Finally, we calculated the gradient shown in Figure 3C by using the same set of 34 significant frontal electrodes. The temporal value of any point shown on the gradient represents the mean significance time of the six nearest electrodes.

Prediction of Decision Content

Can we predict the content of the driver's decision based on a trial-by-trial basis? If so, with which electrodes and at which time point relative to W? To accomplish this, we split the period, spanning 6 to 0 sec before W, into 12 time bins (500 msec each) and performed a leave-one-out (LOO) classification analysis separately for each. Initially, for every trial in each electrode in each time-bin, we computed the average gamma power. Then, in every LOO cross-validation iteration, we selected the two electrodes whose gamma power was most correlated with the training labels (the participant's decisions). We then used the training data gamma power in these two electrodes to train a linear support vector machine (SVM; Cortes & Vapnik, 1995) classifier (using the LIBSVM implementation: http://www.csientu.edu.tw/~cjlin/libsvm). Finally, we used this classifier to classify the content of decision in the current test trial.

The two classes (left or right decision) are unbalanced in some of the patients, such that the chance level is higher than 50%. To avoid biasing the resulting model, we performed a balancing procedure: If one of the classes, in a given training set, contained fewer trials, we increased its size by duplicating randomly selected (with repetition) trials from itself to equalize the amount of trials in the two classes. Importantly, this balancing was performed only on the training data. To account for the variability in this random class balancing procedure, we repeated the cross-validation analysis 10 times for every time bin in every participant, such that the final accuracy result was the average result across these repetitions.

Next, we estimated the p value of each of the 12 time bins, in each participant, by using a permutation test, wherein we shuffled the class labels and repeated the analysis 1,000 times. This generated a null distribution based on random labels, which we used to estimate the one-tailed p value for the given participant.

To correct for the within-subject multiple comparisons originating in the 12 individual time bins, we controlled the within-subject FDR ($q = 0.05$).

In addition to the balancing approach described above, we also tested another balancing approach based on the random removal of trials from the larger class. This balancing approach did not yield at least one significant time bin for each patient. This is probably because of its inherent reduction in the already limited number of trials.

Prediction of Decision Content Using Past Decisions

As suggested by Lages, Boyle, and Jaworska (2013), we attempted to predict the content of the decision using the decisions from previous trials (1 and 2 back). Significant prediction accuracy would indicate that the participants rely on past choices when making new ones. We thus trained, for each participant, linear SVM classifiers to classify the content of the decision using the decisions from one or two previous trials. As before, we tested the classification accuracy using LOO cross-validation and estimated the significance using permutation testing.

Prediction of the Time of the Conscious Decision

In addition to the prediction of the decision content, we carried out another analysis to estimate from which electrodes and how early can we detect the upcoming conscious decision (W). Similar to the approach taken by (Soon et al., 2008), we performed a one-against-one multiclass classification analysis using linear SVM to find which electrodes contained predictive information regarding the timing of W. For each electrode, we divided the iEEG data from each trial, spanning 6 to 0 sec before W, into six 1-sec time bins. Then, we transformed the data from each second into the average power in five frequency bands (delta 1–4, theta 4–7, alpha 8–12, beta 12–30, and gamma 30–100 Hz). Next, for each electrode, we trained and tested SVMs to classify the identity of each of the 6 sec preceding W, using LOO cross-validation. A significantly accurate classification result for one or more of the seconds would demonstrate that, when using the current electrode, it is possible to predict when W will occur. Because there are six possible classes, the chance level is 16.7%.

We then used a 1,000-repetition permutation test to assess the significance of the accuracy results, yielding a null accuracy distribution for each time bin in each electrode, which we used to estimate the p value of the actual classification accuracies and check for significance at an uncorrected threshold of $\alpha = 0.01$.

Instantaneous Prediction in Figure 4

We derived the instantaneous prediction in Figure 4 by summing the weighted gamma activities from two electrodes for the given patient. These electrodes were selected automatically in the aforementioned classification analysis. We defined the gamma activity for time t as the baseline-corrected mean gamma amplitude during t-0.5 sec to t. The weights and intercept used were derived from the linear SVM model described above. The appropriate time to sample the instantaneous prediction is at the end of the earliest significant time bin of the participant (for P05, this is 3.5 sec before W).

RESULTS

While engaging in the driving simulator, patients ($n = 6$) reported making their decision, on average, 5.95 sec (SD = 3.14 sec) after first seeing the junction and, on average,

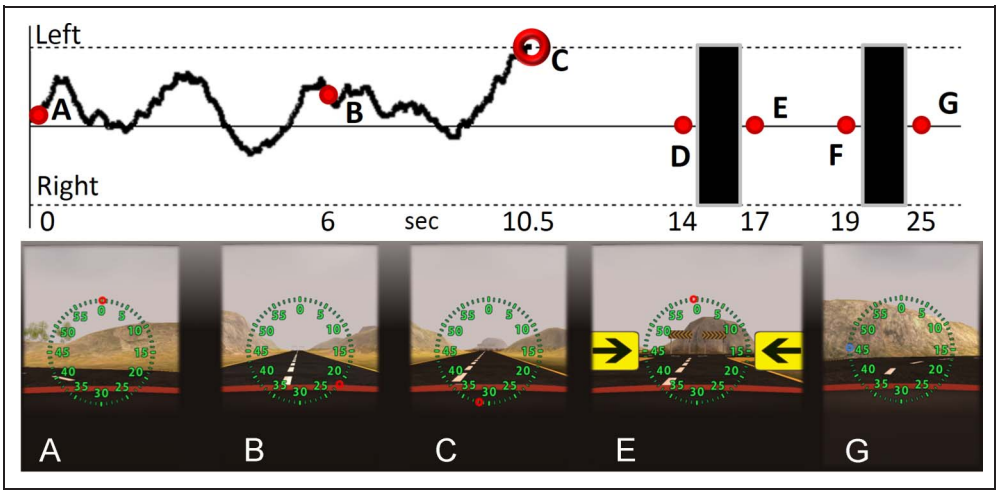

Figure 4. Trial-by-trial prediction. This figure demonstrates the experimental flow of a single actual trial and the instantaneous prediction of the patient's (P05) decision by the classifier (black trace) based on the gamma power in two frontal electrodes (BAs 8 and 9), selected automatically in the classification analysis. (A) Start of the trial, 0 sec. (B) Junction becomes visible, 6 sec. (C) Content of the decision is decoded—the prediction is "left," 10.5 sec. (D)* The actual time of decision as subsequently reported by the patient, 14 sec (see G below). (E) The patient's car arrives at the junction, the mapping arrows appear, and the patient indicates which way to turn, 17 sec. (F)* After pressing the appropriate key, the car turns to the left (in accordance with the prediction), 19 sec. (G) The patient now indicates D as the time of the decision, 25 sec. *Screenshot not shown.

6.06 sec (SD = 3.01 sec) before reaching it. The latter period facilitated the desired decoupling of the motor response from the decision (see Methods and Figure 1). On average, patients committed a motor error in 24.32% of the blocked trials and crashed into the blocker at the junction. Moreover, 75.86% of these crashes occurred when the mapping was inversed.

Spatiotemporal Distribution of Oscillatory Power Preceding Decisions

To identify electrodes that display modulated oscillatory power before left and right decisions and when, we employed a CUMSUM analysis. In this analysis, we compared the average oscillatory power, locked to the reported time of the decision (W), separately for trials in which the patient decided to turn left and trials in which he or she decided to turn right (see Supplementary Figure S1B and Methods).

We focused the CUMSUM analysis on the gamma frequency band (30–100 Hz) because it is thought to represent local multineuron firing rates (Miller, 2010; Whittingstall & Logothetis, 2009; Nir et al., 2007; Liu & Newsome, 2006; Henrie & Shapley, 2005; Lachaux et al., 2005; Siegel & König, 2003) and has recently been suggested to play a causal role in voluntary motor actions (Joundi, Jenkinson, Brittain, Aziz, & Brown, 2012; see Figure 2). Indeed, previous intracranial and MEG studies report changes in gamma band oscillatory power during self-paced movement (Cheyne, Bells, Ferrari, Gaetz, & Bostan, 2008; Pfurtscheller, Graimann, Huggins, Levine, & Schuh, 2003.

In 58 electrodes (of 257 electrodes, 22.57%, from all six patients), the CUMSUM of the difference in gamma band oscillations between left and right decisions was found to be significant ($p < .05$ uncorrected). Six electrodes from two patients were also significant after controlling the within-subject FDR ($q = 0.05$; see Supplementary Figure S2). The median significance time of the CUMSUM of the 58 significant electrodes was 2.45 sec before W (range = 0.1–5.6 sec). The gamma power differences in electrodes that were found to be significant in the permutation test can also be appreciated in the spectrograms of the different choices (left or right) in relation to their respective baselines (see Figure 2).

Figure 3 illustrates the spatial and temporal distribution of the significant electrodes across patients. These results demonstrate that the location of the significant electrodes along a rotated axis with an angle of $\theta = 80.1°$ (approximately parallel to the gradient in Figure 3C; for angle selection criterion, see Methods) was significantly correlated with the electrodes' significance time (Pearson's correlation, $r^2 = .325$, $p < .001$ one-tailed; Figure 3B). Because we determined the gradient by searching for the maximal correlation, this significance value is biased. We thus estimated the significance of this correlation using a permutation test, which also yielded a significant p value ($p < .001$; see Methods). The angle of maximal correlation suggests that electrodes that were significant early are located precentrally in the frontal lobe, and as we approach the reported time of the conscious decision, there is a progression toward anterior and lateral regions of the frontal lobe (see Figure 3C).

The timing and significance level of the electrodes and the direction of the gradient might be sensitive to the specific parametrization of the bounding line. We thus estimated the magnitude of this sensitivity and show that the aforementioned results are robust to the specific parametrization (see Methods).

Note that the clinical determination of electrode placement resulted in asymmetrical coverage of the two hemispheres, thus precluding the examination of hemisphere-specific specialization (i.e., lateralization).

Predicting Decision Content

Can we predict the driver's decision based on neural activity on a trial-by-trial basis? If so, with which electrodes and at which time point relative to W? We performed LOO cross-validation, for each of 12 time bins spanning 6 to 0 sec before W (see Methods). We estimated the p value of each of the 12 time bins, in each participant, by using a permutation test while controlling the within-subject FDR ($q = 0.05$). Each participant had at least one significant time bin (range = [1, 6]). The accuracy range of each patient's most predictive significant time bin was 64.3–82.4%. The time range of each patient's earliest significant time bin was [1, 5.5] sec before W (median = 4.5 sec).

These results demonstrate the ability of gamma power in specific electrodes and at specific time points before W to predict the content of the future decision with considerable accuracy on a trial-by-trial basis. Figure 4 depicts a single trial and the instantaneous decoding of the patient's decision (see Methods).

We repeated this analysis for the blocked trials as well. That is, in each blocked trial, we attempted to predict whether the participant will decide to turn left or right. Interestingly, only one participant had a significant time bin.

In addition to the driver's decision content, we were also able to predict the timing of the decision (W) on a trial-by-trial basis.

Predicting Decision Content Using Past Decisions

To test whether the participants' decisions were impacted by past decisions, we performed 1- and 2-back SVM analyses to predict each trial's decision content using the decisions from previous trials (Lages et al., 2013). Both the 1- and 2-back analyses failed to achieve significance at $\alpha = 0.05$ uncorrected in any of the participants. The mean, across participants, prediction accuracies for the 1- and 2-back analyses were 55.2% and 55.59%, respectively.

Neural Activity Preceding Decision Time

Finally, using time-frequency spectrograms, we examined global changes in oscillation power across frequencies and electrodes (see Methods) in relation to the reported time of the decision in "free" trials, regardless of the content of the decision. We detected effects of power increase or decrease (i.e., event-related synchronization or desynchronization; Pfurtscheller & Lopes da Silva, 1999) in gamma frequency band and also in lower frequency bands (<30 Hz) in relation to W. However, no clear pattern of results emerged over the electrodes and participants.

DISCUSSION

Our results demonstrate that a neural signal predicts the upcoming decision content (up to 5.5 sec) before conscious awareness of the driver's decision-making. The mean accuracy of this prediction on a trial-by-trial basis was considerable, ranging from 64.3% to 82.4%. The predictive neural signal, modulation of power in the gamma-band oscillations, has recently been suggested to be causally related to voluntary motor actions (Joundi et al., 2012) by showing that 70-Hz (within the gamma frequency band) transcranial alternating current stimulation enhances voluntary motor performance. Interestingly, we were not able to predict the decisions in blocked trials. We found only one significant time bin (12) in only one participant. This could be because of the inherent differences in the task, where preconscious activity has no role in the final decision in a blocked trial. Alternatively, it could be simply because of the lower number of trials, as only ~30% of trials were blocked.

The spatiotemporal gradient in the CUMSUM analysis indicates that decision content is available earlier in dorsal premotor regions and later in more anterior and lateral frontal regions, suggesting an early preconscious role for the premotor cortices in the decision-making/action-selection process. This is compatible with the suggestion that it is the accumulation of ongoing neuronal activity in premotor cortices (e.g., SMA) together with parietal regions that supports the feeling of conscious intention (Fried et al., 2011; Haggard, 2011; Matsuhashi & Hallett, 2008; Gold & Shadlen, 2007; Libet, Gleason, et al., 1983). This is also in accordance with previous studies showing that some decisions can be discriminated based on early activity in motor and perceptual (e.g., FEFs and lateral intraparietal cortex) regions (Kim & Basso, 2008, 2010; Scherberger & Andersen, 2007) or that failure of response inhibition can be predicted from oscillatory changes in sensorimotor cortices and occipital regions (Bengson, Mangun, & Mazaheri, 2012; Mazaheri, Nieuwenhuis, van Dijk, & Jensen, 2009). In the decision-making process, the role of anterior frontal and parietal regions has been demonstrated in studies by Koechlin (e.g., Kouneiher, Charron, & Koechlin, 2009; Koechlin & Hyafil, 2007), Shallice (e.g., Picton et al., 2007; Vallesi et al., 2007), and others (e.g., Krieghoff, 2009; Pesaran, Nelson, & Andersen, 2008; Deiber, Ibanez, Sadato, & Hallett, 1996). Of note is that, based on local patterns of fMRI signals in frontopolar and medial parietal regions (Soon et al., 2008, 2013), reported earliest decoding of decision content as early as 4–7 sec before the reported time of decision (albeit at relatively low accuracy rates). In contrast with fMRI, the current study utilized iEEG, which offers better time resolution. This enhanced time resolution enabled us to characterize the spatiotemporal gradient.

Interestingly, as can be seen in Figure 3, the CUMSUM analysis detected significant electrodes in the temporal cortex. This is of no surprise considering that the current task significantly engages such cognitive capacities as memory, attention, and spatial navigation, which in turn involve temporal regions.

A central challenge in the interpretation of the bulk of the related studies (Trevena & Miller, 2009; Soon et al.,

2008; Haggard & Eimer, 1999; Libet, Gleason, et al., 1983) is the potential confounding of decision content by motor preparation (Hampton & O'Doherty, 2007; Haynes et al., 2007). The current study was specifically designed to disambiguate the two (see Methods and Figure 1) and therefore separate proximal intentions from motor intentions (Pacherie, 2008). Thus, the early neuronal signal reflecting the future driver's decision in our study should not be viewed as motor preparation, as the instruction of which hand to use to signal the decision was decoupled from the desired direction of the turn. Furthermore, by using 1- and 2-back SVM classification analysis, we show that the participants' decisions were not significantly affected by past decisions. This implies that the participants' decisions were indeed free and unpredictable (Lages et al., 2013).

The behavioral results indicate that our knowledge of the participants' actual left/right decisions is not accurate. This is because of the fact that the patients performed motor errors, on average, in 24.23% of the blocked trials and crashed into the blocker. This amount of motor errors is not negligible and can only be explained by the fact that the patients had only 5 sec to respond from the moment the mapping appeared. This period may be too brief for such patients with chronic epilepsy who are also recovering from recent surgical implantation of the iEEG electrodes. This is underlined when we consider the fact that, of these crashed trials, 75.86% took place when the key mapping was inversed and was thus more cognitively demanding. This lack of certainty regarding the content of the patients' decisions places an upper bound on the accuracy achievable when trying to predict the content of the decision.

The current study relies on the patients' reported time of decision (W) to infer decision time. Yet, research has shown that preconscious effects can be produced as a result of participants simply not reporting the contents of their awareness accurately (Bengson & Hutchison, 2007). Further research has demonstrated that subjective report of W is prone to errors and biases (e.g., Joordens, van Duijn, & Spalek, 2002) and has suggested against using subjective reports of time of awareness as measures of awareness (Banks & Isham, 2009). It is possible that, in the current study, participants did not report the earliest time of conscious awareness of the decision but rather the time in which they became fully confident of their decision. This would imply that the classifier actually capitalized on conscious decision-making processes that took place before the reported time of decision. However, Fried and colleagues showed that shifting W back by more than 200 msec significantly reduces the number of significant units detected (Fried et al., 2011), indicating that the neural activity predating the reported time of conscious decision is fairly localized in time. Because the time scales in the current experiment are fairly long, in the order of seconds, it is likely that the current reported time of decision is at least partially correlated to the actual initial conscious awareness of the decision.

A limitation of the current study that is shared with other similar studies (e.g., Soon et al., 2008, 2013; Haggard & Eimer, 1999; Libet, Gleason, et al., 1983) is the fact that the participants' decisions entailed no risk or value (Lavazza & De Caro, 2009), two major aspects of naturalistic decision-making. However, it is not clear whether any experimental design could overcome this limitation and still allow for free decisions. If the participants' decisions do have value, then prediction of the participant's decision will necessarily confound value representation with abstract representation of the decision content.

A final limitation of the current study is related to eye movements, which we did not collect. It is conceivable that, before making left or right decisions, participants perform consistent eye movements, leading to consistent neural activity. Such neural activity may then underlie the results reported above. This suggests that eye movement tracking could aid future investigations in this field.

Although we extracted the present neuronal measure from intracranial electrodes, future studies will be needed to determine if noninvasive recordings from leads placed on the scalp yield predictive measures as well. Such findings, and specifically the trial-by-trial prediction, may herald development of brain–computer interfaces, in which the user's intentions are decoded before conscious awareness. This could increase the speed with which action intentions are transmitted through the interface into actual actions or when indicated, into modification or even prevention of such actions. The scientific, technological, and societal implications of such interfaces remain open for debate.

Acknowledgments

We thank the patients for volunteering to take part in the study. We thank Drs. U. Kramer, S. Kippervasser, M. Neufeld, and F. Andelman; D. Josef, S. Nagar, R. Cohen, C. Yosef, G. Yehezkel; and the EEG technicians at the Tel Aviv Medical Center for assistance. We thank Y. Benjamini for statistical consultation. We also thank M. Harel for MRI electrode reconstruction. This study was funded by the Israel Science Foundation grant to I. F.; Intel grant 015008 to Y. Y.; Converging Technologies fellowship granted by the Israeli Council for Higher Education to O. P. and the Dana foundation; Lady Davis fellowship to A. T.; ICORE Higher Education Center grant to R. M., I. F., and Y. Y.; and L. and L. Richmond Research Fund.

Reprint requests should be sent to Itzhak Fried, Department of Surgery/Neurosurgery, UCLA, Box 957039, 740 Westwood Plaza, Los Angeles, CA 90095-7039, or via e-mail: ifried@mednet.ucla.edu.

REFERENCES

Armitage, P. (1975). *Sequential medical trials* (2nd ed.). Oxford: Blackwell.

Assal, F., Schwartz, S., & Vuilleumier, P. (2007). Moving with or without will: Functional neural correlates of alien hand syndrome. *Annals of Neurology, 62,* 301–306.

Banks, W. P., & Isham, E. A. (2009). We infer rather than perceive the moment we decided to act. *Psychological Science, 20,* 17–21.

Basar, E., Basar-Eroglu, C., Karakas, S., & Schürmann, M. (2001). Gamma, alpha, delta, and theta oscillations govern cognitive processes. *International Journal of Psychophysiology, 39,* 241–248.

Bengson, J. J., & Hutchison, K. A. (2007). Variability in response criteria affects estimates of conscious identification and unconscious semantic priming. *Consciousness and Cognition, 16,* 785–796.

Bengson, J. J., Mangun, G. R., & Mazaheri, A. (2012). The neural markers of an imminent failure of response inhibition. *Neuroimage, 59,* 1534–1539.

Brass, M., & Haggard, P. (2007). To do or not to do: The neural signature of self-control. *Journal of Neuroscience, 27,* 9141–9145.

Cheyne, D., Bells, S., Ferrari, P., Gaetz, W., & Bostan, A. C. (2008). Self-paced movements induce high-frequency gamma oscillations in primary motor cortex. *Neuroimage, 42,* 332–342.

Cortes, C., & Vapnik, V. (1995). Support-vector networks. *Machine Learning, 20,* 273–297.

Deiber, M. P., Ibanez, V., Sadato, N., & Hallett, M. (1996). Cerebral structures participating in motor preparation in humans: A positron emission tomography study. *Journal of Neurophysiology, 75,* 233–247.

Delorme, A., & Makeig, S. (2004). EEGLAB: An open source toolbox for analysis of single-trial EEG dynamics including independent component analysis. *Journal of Neuroscience Methods, 134,* 9–21.

Desmurget, M., Reilly, K. T., Richard, N., Szathmari, A., Mottolese, C., & Sirigu, A. (2009). Movement intention after parietal cortex stimulation in humans. *Science, 324,* 811–813.

Desmurget, M., & Sirigu, A. (2009). A parietal-premotor network for movement intention and motor awareness. *Trends in Cognitive Sciences, 13,* 411–419.

Fried, I., Mukamel, R., & Kreiman, G. (2011). Internally generated preactivation of single neurons in human medial frontal cortex predicts volition. *Neuron, 69,* 548–562.

Gold, J. I., & Shadlen, M. N. (2007). The neural basis of decision making. *Annual Review of Neuroscience, 30,* 535–574.

Gomes, G. (1998). The timing of conscious experience: A critical review and reinterpretation of Libet's research. *Consciousness and Cognition, 7,* 559–595.

Gomes, G. (2007). Free will, the self, and the brain. *Behavioral Sciences & the Law, 25,* 221–234.

Gomes, G. (2010). Preparing to move and deciding not to move. *Consciousness and Cognition, 19,* 457–459.

Haggard, P. (2005). Conscious intention and motor cognition. *Trends in Cognitive Sciences, 9,* 290–295.

Haggard, P. (2008). Human volition: Towards a neuroscience of will. *Nature Reviews Neuroscience, 9,* 934–946.

Haggard, P. (2011). Decision time for free will. *Neuron, 69,* 404–406.

Haggard, P., & Eimer, M. (1999). On the relation between brain potentials and the awareness of voluntary movements. *Experimental Brain Research, 126,* 128–133.

Hampton, A. N., & O'Doherty, J. P. (2007). Decoding the neural substrates of reward-related decision making with functional MRI. *Proceedings of the National Academy of Sciences, U.S.A., 104,* 1377–1382.

Haynes, J.-D., Sakai, K., Rees, G., Gilbert, S., Frith, C., & Passingham, R. E. (2007). Reading hidden intentions in the human brain. *Current Biology, 17,* 323–328.

Hedgcock, W., Crowe, D., Leuthold, A., & Georgopoulos, A. (2009). A magnetoencephalography study of choice bias. *Experimental Brain Research, 202,* 121–127.

Henrie, J. A., & Shapley, R. (2005). LFP power spectra in V1 cortex: The graded effect of stimulus contrast. *Journal of Neurophysiology, 94,* 479–490.

Joordens, S., van Duijn, M., & Spalek, T. M. (2002). When timing the mind one should also mind the timing: Biases in the measurement of voluntary actions. *Consciousness and Cognition, 11,* 231–240.

Joundi, R. A., Jenkinson, N., Brittain, J.-S., Aziz, T. Z., & Brown, P. (2012). Driving oscillatory activity in the human cortex enhances motor performance. *Current Biology, 22,* 403–407.

Keller, I., & Heckhausen, H. (1990). Readiness potentials preceding spontaneous motor acts: Voluntary vs. involuntary control. *Electroencephalography and Clinical Neurophysiology, 76,* 351–361.

Kim, B., & Basso, M. A. (2008). Saccade target selection in the superior colliculus: A signal detection theory approach. *Journal of Neuroscience, 28,* 2991–3007.

Kim, B., & Basso, M. A. (2010). A probabilistic strategy for understanding action selection. *Journal of Neuroscience, 30,* 2340–2355.

Koechlin, E., & Hyafil, A. (2007). Anterior prefrontal function and the limits of human decision-making. *Science, 318,* 594–598.

Kornhuber, H. H., & Deecke, L. (1965). Hirnpotentialänderungen bei willkürbewegungen und passiven bewegungen des menschen: Bereitschaftspotential und reafferente potentiale. *Pflügers Archiv: European Journal of Physiology, 284,* 1–17.

Kouneiher, F., Charron, S., & Koechlin, E. (2009). Motivation and cognitive control in the human prefrontal cortex. *Nature Neuroscience, 12,* 939–945.

Krieghoff, V. (2009). Dissociating what and when of intentional actions. *Frontiers in Human Neuroscience, 3,* 3.

Lachaux, J.-P., George, N., Tallon-Baudry, C., Martinerie, J., Hugueville, L., Minotti, L., et al. (2005). The many faces of the gamma band response to complex visual stimuli. *Neuroimage, 25,* 491–501.

Lages, M., Boyle, S. C., & Jaworska, K. (2013). Flipping a coin in your head without monitoring outcomes? Comments on predicting free choices and a demo program. *Decision Neuroscience, 4,* 925.

Lavazza, A., & De Caro, M. (2009). Not so fast. On some bold neuroscientific claims concerning human agency. *Neuroethics, 3,* 23–41.

Libet, B. (2004). *Mind time*. Cambridge, MA: Harvard University Press.

Libet, B., Gleason, C. A., Wright, E. W., & Pearl, D. K. (1983). Time of conscious intention to act in relation to onset of cerebral activity (readiness-potential): The unconscious initiation of a freely voluntary act. *Brain, 106,* 623–642.

Libet, B., Wright, E. W., & Gleason, C. A. (1983). Preparation- or intention-to-act, in relation to pre-event potentials recorded at the vertex. *Electroencephalography and Clinical Neurophysiology, 56,* 367–372.

Liu, J., & Newsome, W. T. (2006). Local field potential in cortical area MT: Stimulus tuning and behavioral correlations. *The Journal of Neuroscience, 26,* 7779–7790.

Matsuhashi, M., & Hallett, M. (2008). The timing of the conscious intention to move. *European Journal of Neuroscience, 28,* 2344–2351.

Mazaheri, A., Nieuwenhuis, I. L. C., van Dijk, H., & Jensen, O. (2009). Prestimulus alpha and mu activity predicts failure to inhibit motor responses. *Human Brain Mapping, 30,* 1791–1800.

Miller, K. J. (2010). Broadband spectral change: Evidence for a macroscale correlate of population firing rate? *Journal of Neuroscience, 30,* 6477–6479.

Nir, Y., Fisch, L., Mukamel, R., Gelbard-Sagiv, H., Arieli, A., Fried, I., et al. (2007). Coupling between neuronal firing rate,

gamma LFP, and BOLD fMRI is related to interneuronal correlations. *Current Biology, 17,* 1275–1285.
Oppenheim, A. V., & Schafer, R. W. (2009). *Discrete-time signal processing*. Englewood Cliffs, NJ: Prentice Hall Press.
Pacherie, E. (2008). The phenomenology of action: A conceptual framework. *Cognition, 107,* 179–217.
Pesaran, B., Nelson, M. J., & Andersen, R. A. (2008). Free choice activates a decision circuit between frontal and parietal cortex. *Nature, 453,* 406–409.
Pfurtscheller, G., Graimann, B., Huggins, J. E., Levine, S. P., & Schuh, L. A. (2003). Spatiotemporal patterns of beta desynchronization and gamma synchronization in corticographic data during self-paced movement. *Clinical Neurophysiology, 114,* 1226–1236.
Pfurtscheller, G., & Lopes da Silva, F. H. (1999). Event-related EEG/MEG synchronization and desynchronization: Basic principles. *Clinical Neurophysiology, 110,* 1842–1857.
Picton, T. W., Stuss, D. T., Alexander, M. P., Shallice, T., Binns, M. A., & Gillingham, S. (2007). Effects of focal frontal lesions on response inhibition. *Cerebral Cortex, 17,* 826–838.
Privman, E., Nir, Y., Kramer, U., Kipervasser, S., Andelman, F., Neufeld, M. Y., et al. (2007). Enhanced category tuning revealed by intracranial electroencephalograms in high-order human visual areas. *Journal of Neuroscience, 27,* 6234–6242.
Scherberger, H., & Andersen, R. A. (2007). Target selection signals for arm reaching in the posterior parietal cortex. *Journal of Neuroscience, 27,* 2001–2012.
Shibasaki, H., & Hallett, M. (2006). What is the Bereitschaftspotential? *Clinical Neurophysiology, 117,* 2341–2356.
Siegel, M., & König, P. (2003). A functional gamma-band defined by stimulus-dependent synchronization in area 18 of awake behaving cats. *The Journal of Neuroscience, 23,* 4251–4260.
Sirigu, A., Daprati, E., Ciancia, S., Giraux, P., Nighoghossian, N., Posada, A., et al. (2004). Altered awareness of voluntary action after damage to the parietal cortex. *Nature Neuroscience, 7,* 80–84.
Soon, C. S., Brass, M., Heinze, H.-J., & Haynes, J.-D. (2008). Unconscious determinants of free decisions in the human brain. *Nature Neuroscience, 11,* 543–545.
Soon, C. S., He, A. H., Bode, S., & Haynes, J.-D. (2013). Predicting free choices for abstract intentions. *Proceedings of the National Academy of Sciences, U.S.A., 110,* 6217–6222.
Stockwell, R. G., Mansinha, L., & Lowe, R. P. (1996). Localization of the complex spectrum: The S transform. *IEEE Transactions on Signal Processing, 44,* 998–1001.
Trevena, J., & Miller, J. (2009). Brain preparation before a voluntary action: Evidence against unconscious movement initiation. *Consciousness and Cognition, 19,* 447–456.
Vallesi, A., Mussoni, A., Mondani, M., Budai, R., Skrap, M., & Shallice, T. (2007). The neural basis of temporal preparation: Insights from brain tumor patients. *Neuropsychologia, 45,* 2755–2763.
Wegner, D. M. (2003). The mind's best trick: How we experience conscious will. *Trends in Cognitive Sciences, 7,* 65–69.
Whittingstall, K., & Logothetis, N. K. (2009). Frequency-band coupling in surface EEG reflects spiking activity in monkey visual cortex. *Neuron, 64,* 281–289.